

## Balancing life with glycoconjugates: Monitoring unfolded protein response-mediated anti-angiogenic action of tunicamycin by Raman spectroscopy\*

Maria O. Longas<sup>1,†</sup>, Ashok Kotapati<sup>1</sup>, Kilari PVRK Prasad<sup>2</sup>,  
Aditi Banerjee<sup>3,†</sup>, Jesus Santiago<sup>3</sup>, Krishna Bakshi<sup>4</sup>, and  
Dipak K. Banerjee<sup>3,5,‡</sup>

<sup>1</sup>*Department of Chemistry and Physics, Purdue University Calumet, Hammond, IN 46323-2094, USA;* <sup>2</sup>*Department of Computer and Information Technology, Purdue University Calumet, Hammond, IN 46323-2094, USA;* <sup>3</sup>*Department of Biochemistry, School of Medicine, University of Puerto Rico, Medical Sciences Campus, San Juan, PR 00936-5067, USA;* <sup>4</sup>*Department of Anatomy and Cell Biology, Universidad Central del Caribe, Bayamon, PR 00960-3001, USA;* <sup>5</sup>*Institute of Functional Nanomaterials, University of Puerto Rico, Rio Piedras Campus, San Juan, PR 00931-1907, USA*

**Abstract:** Asparagine-linked protein glycosylation is a hallmark for glycoprotein structure and function. Its impairment by tunicamycin [a competitive inhibitor of *N*-acetylglucosaminyl 1-phosphate transferase (GPT)] has been known to inhibit neo-vascularization (i.e., angiogenesis) in humanized breast tumor due to an induction of endoplasmic reticulum (ER) stress-mediated unfolded protein response (UPR). The studies presented here demonstrate that (i) tunicamycin inhibits capillary endothelial cell proliferation in a dose-dependent manner; (ii) treated cells are incapable of forming colonies upon its withdrawal; and (iii) tunicamycin treatment causes nuclear fragmentation. Tunicamycin-induced ER stress-mediated UPR event in these cells was studied with the aid of Raman spectroscopy, in particular, the interpretation of bands at 1672, 1684, and 1694 cm<sup>-1</sup>, which are characteristics of proteins and originate from C=O stretching vibrations of mono-substituted amides. In tunicamycin-treated cells, these bands decreased in area as follows: at 1672 cm<sup>-1</sup> by 41.85 % at 3 h and 55.39 % at 12 h; at 1684 cm<sup>-1</sup> by 20.63 % at 3 h and 40.08 % at 12 h; and also at 1994 cm<sup>-1</sup> by 33.33 % at 3 h and 32.92 % at 12 h, respectively. Thus, in the presence of tunicamycin, newly synthesized protein chains fail to arrange properly into their final secondary and/or tertiary structures, and the random coils they form had undergone further degradation.

**Keywords:** angiogenesis; antibiotics; anticancer activity; asparagine-linked glycoproteins; breast cancer; enzyme inhibitors; endoplasmic reticulum (ER) stress; nucleosides; proteins; Raman spectroscopy; tunicamycin; unfolded protein response.

---

\**Pure Appl. Chem.* **84**, 1837–1937 (2012). A collection of invited papers based on presentations on the Chemistry of Life theme at the 43<sup>rd</sup> IUPAC Congress, San Juan, Puerto Rico, 30 July–7 August 2011.

<sup>†</sup>Contributed equally to paper.

<sup>‡</sup>Corresponding author: Tel.: (787) 758-2525 Ext. 1624; Fax: (787) 274-8724; E-mail: dipak.banerjee@upr.edu

## INTRODUCTION

Glycans are modifications of proteins (glycoproteins and proteoglycans) or lipids (glycosphingolipids) and form the core structure of the glycosphosphatidylinositol (GPI) anchors responsible for anchoring proteins to the membrane [1,2]. The roles of glycans are diverse. They contribute to the folding and conformational stability of many proteins [3–5], mediate host–pathogen interactions and aspects of innate immunity [6–9], and serve as ligands for glycan-binding proteins that mediate cell trafficking, cell adhesion, and cell signaling [10–15].

The biosynthetic enzymes responsible for synthesizing the core regions of *N*- and *O*-linked oligosaccharides are ubiquitously expressed, whereas glycosyltransferases that elaborate terminal structures are expressed in a highly tissue-specific manner, accounting for tissue- and ultimately cell-type-specific glycosylation. Aberrant glycosylation occurs in essentially all types of experimental and human cancers, and many glycosyl epitopes constitute tumor-associated antigens [16]. A long-standing debate has been whether aberrant glycosylation is a result or a cause of cancer. Many recent studies indicate that some, if not all, aberrant glycosylation is a result of initial oncogenic transformation, as well as a key event in induction of invasion and metastasis. High expression of some glycosyl epitopes promotes invasion and metastasis, leading to shorter 5–10 year survival rates of patients. By contrast, expression of some other glycosyl epitopes suppresses tumor progression, leading to higher postoperative survival rates [17,18]. The former category of epitopes include  $\beta$ 6GlcNAc branching in *N*-linked (asparagine-linked) structure; sialyl-Tn in *O*-linked (serine/threonine-linked) structure; sialyl-Le<sup>x</sup>, sialyl-Le<sup>a</sup>, and Le<sup>y</sup> in either *N*-, *O*-, or lipid-linked structure; GM2, GD3, and sialyl-Gb5 in lipid-linked structure. The latter category includes  $\beta$ 4GlcNAc competitive with  $\beta$ 6GlcNAc; histo-blood group A and B competitive with sialylated structures including sialyl-Le<sup>x</sup> and sialyl-Le<sup>a</sup>; Gb5 competitive with sialyl-Gb5. The expression mechanism of these glycosyl epitopes in terms of status of respective glycosyltransferase genes has been extensively studied [19,20].

About one-third of newly synthesized proteins translocate to the lumen of the endoplasmic reticulum (ER) where they are post-translationally modified and folded into correct 3D structures before being targeted to various cellular organelles or transported to the surface of the cell. One of these post-translational modifications includes glycosylation of the asparagine residue (*N*-linked) when present in a tripeptide sequence Asn-X-Ser/Thr. Physiological states that increase the demand for protein folding, or stimuli that disrupt the reactions by which proteins fold, create an imbalance between the protein-folding load and the capacity of the ER, causing unfolded or misfolded proteins to accumulate in the ER lumen—a condition referred to as “ER stress”. To ensure the fidelity of protein folding and to prevent ER stress, eukaryotic cells have evolved a set of intracellular pathways that signal the presence of cellular stress called unfolded protein response (UPR), which alters the ability of cells transcriptional and translational programs to cope with stressful conditions and to resolve the protein-folding defect [21,22].

Angiogenesis (i.e., proliferation and differentiation of capillary endothelial cells) is essential for breast and other solid tumor progression and metastasis. Asparagine-linked glycoproteins have been found to play an important role in capillary endothelial cell proliferation and differentiation [23,24]. Furthermore, “hybrid”- but not “complex”-type glycans are required for capillary tube formation [25–27]. One of our objectives has been to target the cellular machinery for protein *N*-glycosylation and develop anti-angiogenic glycotherapeutic(s) to treat breast cancer. Using a glucosamine-containing pyrimidine nucleoside tunicamycin, we have recently shown that the process of neo-vascularization is irreversible by exogenous addition of vascular endothelial growth factor-165 (VEGF<sub>165</sub>), and down-regulation of phosphotyrosine kinase activity correlates well with reduced phosphorylation of VEGFR1 and VEGFR2 receptors. In vivo experiments indicate tunicamycin inhibits neo-vascularization in Matrigel™ implant in *Balb/c (nu/nu)* mice and reduces a double- and triple-negative breast tumor progression by ~55 to 65 % of humanized breast tumors in orthotopic and/or xenograft models in nude

mice [28]. The molecular mechanisms indicate development of ER stress in tunicamycin-treated tumor microvasculature causing UPR-mediated apoptotic death [28].

To study the intracellular proteins status under ER stress, we have used Raman spectroscopy since it characterizes normal and distorted proteins and can monitor cell death *in vitro* [29–32]. The decrease of characteristic Raman bands in tunicamycin-treated cells indicates failure of newly synthesized proteins to arrange into their secondary and/or tertiary structures.

## **MATERIALS AND METHODS**

### **Materials**

Hydroxyurea, dimethylsulfoxide, nystatin, ethidium bromide, and tunicamycin were obtained from Sigma Aldrich (St. Louis, MO). Mouse monoclonal antibody for actin was from BD-Bioscience (San Diego, CA). Rabbit polyclonal antibody for GRP-78 was from Santa Cruz Biotechnology (Santa Cruz, CA). HRP-conjugated goat anti-rabbit IgG/anti-mouse IgG, streptavidin, ECL chemiluminescence detection kit were from GE Healthcare (Piscataway, NJ). TRIzol was from Invitrogen Life Technologies (Carlsbad, CA). All cell culture wares were from Sarstedt (Newton, NC) and the fetal bovine serum was purchased from HyClone Laboratories (Logan, UT). All other chemicals and solvents used were of the highest purity available.

### **Cell line**

The capillary endothelial cells were from the laboratory stock of a non-transformed capillary endothelial cell line from bovine adrenal medulla [33].

### **Culturing of capillary endothelial cells and treating with tunicamycin**

Capillary endothelial cells were maintained and synchronized as previously described [33,34]. Tunicamycin (1  $\mu\text{g}/\text{ml}$ ) was added in Eagle's minimum essential medium with Earle's salts (EMEM) containing 2 % (v/v) fetal bovine serum (heat-inactivated) for 0–32 h. The cells were cultured at 37 °C in a humidified incubator containing 95 % air and 5 %  $\text{CO}_2$ .

### **MTT assay for cell proliferation**

Cells were suspended in complete EMEM containing 10 % fetal bovine serum.  $1.6 \times 10^4$  cells in 200  $\mu\text{l}$  were plated in 96 well plates. After culturing for 24 h, the cells were synchronized and treated with tunicamycin (1  $\mu\text{g}/\text{ml}$ ) as described before [34]. At an interval of 24 h, media were removed and the cells were washed three times with phosphate-buffered saline (PBS), pH 7.2. MTT (2 mg/ml) was added in each well, and the cells were incubated for 4 h at 37 °C. At the end of incubation, MTT was removed and 200  $\mu\text{l}$  10 % dimethyl sulfoxide (DMSO) was added. After 10 min, the plates were read at 550 nm in EIA plate reader (Bio-Rad).

### **Qualitative and quantitative monitoring of apoptosis**

Apoptotic changes were quantified by Hoechst 33258 (Molecular Probes) staining of nuclei. Cells were cultured, synchronized, and treated with tunicamycin (1  $\mu\text{g}/\text{ml}$ ) as mentioned above. At the end of the treatment, the cells were harvested by trypsinization, fixed with 4 % (v/v) formaldehyde in PBS, pH 7.2 for 15 min [36], washed, resuspended in 70 % (v/v) ethanol and stored at –20 °C until use. Cells were washed twice again in PBS, pH 7.2, and stained with 50  $\mu\text{l}$  of Hoechst 33528 (10  $\mu\text{g}/\text{ml}$  in PBS, pH 7.2). Following 15 min incubation at room temperature, 15  $\mu\text{l}$  aliquot was placed on a glass slide,

and 500 stained nuclei were counted under a fluorescence microscope (Zeiss AXIO). Each experiment was repeated three times, and in each experimental condition, more than 1000 single cells were scored for apoptosis.

### Single-cell clonogenic assay

Capillary endothelial cells ( $2 \times 10^6$  cells) were seeded in 75 cm<sup>2</sup> flasks and cultured for 24 h at 37 °C in a humidified incubator in the presence of 95 % air and 5 % CO<sub>2</sub> in complete EMEM containing 10 % fetal bovine serum. The cells were synchronized for 72 h and treated with tunicamycin (1 µg/ml) for 32 h as described before [35]. Tunicamycin-treated cells were trypsinized, and 5000 cells were dispersed per well in 6 well clusters and incubated at 37 °C in complete EMEM containing 10 % fetal bovine serum. The cells were monitored for 9 days with changing media every third day. At the conclusion of the incubation period, the media were removed and the cells were stained with 0.5 % crystal violet in methanol for 1 h at room temperature. Images were collected in a Nikon ATM microscope, and the cell numbers in five randomly selected colonies were counted.

### Raman spectroscopy

Capillary endothelial cells were synchronized and cultured in the presence or absence of tunicamycin (1 µg/ml). At the times indicated, cell growth was interrupted, cells were removed from culture dishes with a short trypsinization, washed thoroughly with PBS, pH 7.4, suspended in 70 % aqueous ethanol (v/v), allowed to stand at -20 °C for 2 days, and recovered by centrifugation. Pellets containing around  $3.7 \times 10^4$  cells were placed in a micro-cup, and ethanol was allowed to evaporate at room temperature. Raman spectra were recorded using an R 2001 Raman Systems Spectrophotometer from Ocean Optics. Cells were scanned in the 2800–0 cm<sup>-1</sup> range, at integration 400, average 1 and box 15. Raman bands were quantified using Spectrum 1000 software from Perkin Elmer.

### Statistical analysis

Statistical analysis was carried out with Graph Pad Prism 4 software (Graph Pad Software Inc., San Diego, CA). Quantitative data are presented as mean plus standard error (SE). Mean  $\pm$  SE was calculated by one-way analysis of variance (ANOVA). Significance between groups was further analyzed using the post-hoc Tukey's test.

## RESULTS

### Tunicamycin inhibits capillary endothelial cell proliferation

Proliferation and differentiation of capillary endothelial cells into capillaries are essential for neo-vascularization during tumor progression and metastasis. It has been proposed earlier that “hybrid”- but not “complex”-type *N*-glycans are required for capillary tube formation [24], but the question remained about the status of the angiogenesis when protein *N*-glycosylation is inhibited. To address such a question, we have used a potent *N*-glycosylation inhibitor, tunicamycin on the proliferation of a non-transformed capillary endothelial cell line in culture. We have performed MTT assay on these cells after treating them with tunicamycin (0–2 µg/ml) over a period of 120 h. The results in Fig. 1 confirmed that at 0.25 µg/ml tunicamycin had no effect on the cellular proliferation after 24 h, whereas at 0.5 µg/ml it inhibited ~14.2 %, but at 1.0–2.0 µg/ml the inhibition was approximately 21.4 %. The inhibition, however, continued to rise with the time of treatment. For example, it was approximately 21.4 % at tunicamycin concentration 0.25–0.5 µg/ml and approximately 50 % at 1.0–2.0 µg/ml after 48 h of treat-

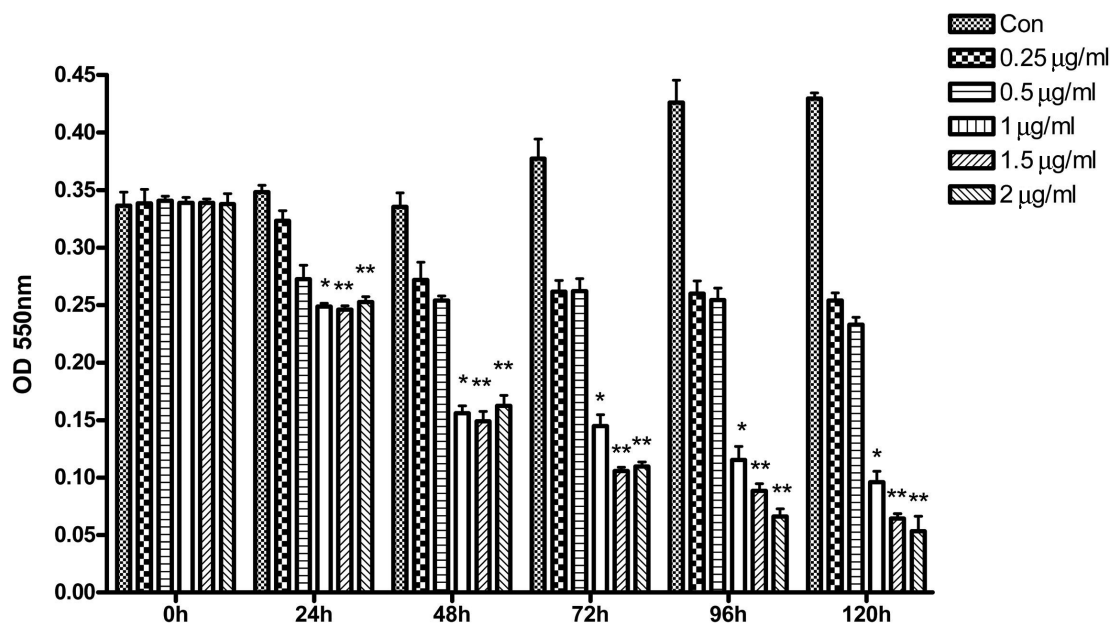


**Fig. 1** Tunicamycin inhibits capillary endothelial cell proliferation.  $1.6 \times 10^4$  cells in EMEM containing 10 % fetal bovine serum in 200  $\mu$ l were plated in 96 well plates. After 24 h, the cells were synchronized and treated with tunicamycin (1  $\mu$ g/ml) as in Materials and Methods. Cells were removed after every 24 h, washed with PBS, pH 7.2, and incubated with MTT (2 mg/ml) for 4 h at 37 °C. At the end of incubation, MTT was removed and 200  $\mu$ l 10 % DMSO was added. After 10 min the plates were read at 550 nm in EIA plate reader (Bio Rad). \* =  $p < 0.01$ ; \*\* =  $p < 0.001$ .

ment. These values were changed to approximately 31.2 and 62.5–68.7 %, respectively, after 72 h of treatment, and increased much more at later time points.

### Tunicamycin-treated cells are less likely to form colonies

The ability to form colonies has been observed more frequently in cells with epithelial characteristics but other cell types are also known to form colonies. To evaluate the colony-forming ability, the capillary endothelial cells treated with tunicamycin (1  $\mu$ g/ml) for 3 and 32 h were lifted, replated, and cultured for 9–14 days in EMEM containing 10 % (v/v) fetal bovine serum. The results in Fig. 2 explain that cells treated with tunicamycin for 3 or 32 h have lost their ability to form colonies. On the other hand, the control cells have retained such ability.

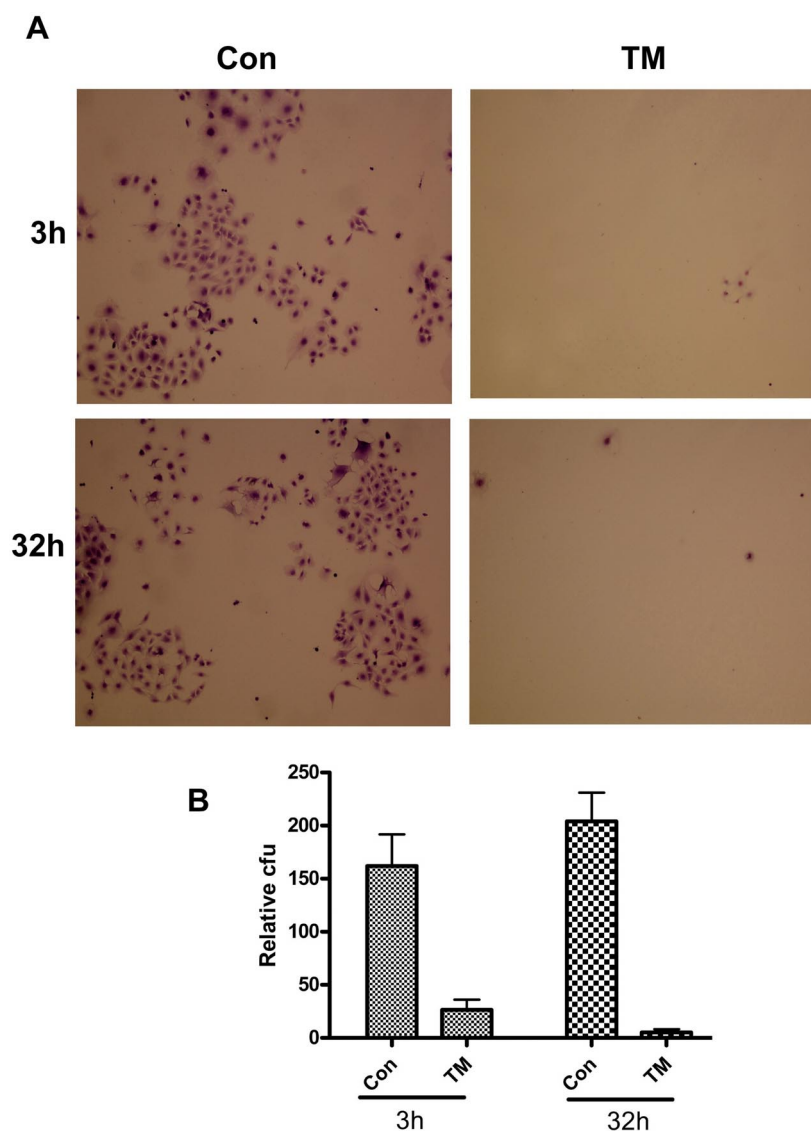


**Fig. 2** Tunicamycin-treated cells are less likely to form colonies. Capillary endothelial cells ( $2 \times 10^6$  cells) were cultured for 24 h at 37 °C in the presence of 95 % air and 5 % CO<sub>2</sub> in a humidified incubator and synchronized as in Materials and Methods. After treating them with tunicamycin (1 µg/ml for 32 h) 5000 cells were disbursed per well in 6 well clusters and incubated at 37 °C in complete EMEM with 10 % fetal bovine serum. The cells were monitored for 9 days with changing media every second day. At the end, the media were removed and the cells were stained with 0.5 % crystal violet in methanol for 1 h at room temperature. Images were collected in a Nikon ATM microscope, and the cell numbers in five randomly selected colonies were counted. The results are expressed as mean  $\pm$  SE. A: photomicrographs, Con = control; TM = tunicamycin; B: quantification of colonies, Con = control; TM = tunicamycin.

### Tunicamycin-treated cells undergo nuclear fragmentation

Reduction of cellular proliferation is associated with either a cell cycle arrest or a cell death or a combination of the two. In our earlier report [34], we have indicated not only that there is a cell cycle arrest in G1 but also a loss of cell numbers with time due to cell death in tunicamycin-treated capillary

endothelial cells. To evaluate the nature of cell death we have stained the nuclei from control and tunicamycin (1  $\mu\text{g/ml}$ )-treated cells with Hoechst 33528 (10  $\mu\text{g/ml}$  in PBS, pH 7.2) and examined them under a fluorescence microscope. The photomicrographs of the nuclei from tunicamycin-treated cells exhibited fragmentation (arrows) with no changes occurring in untreated controls (Fig. 3). Thus, confirming that tunicamycin treatment induces apoptotic death (i.e., programmed cell death) of capillary endothelial cells.

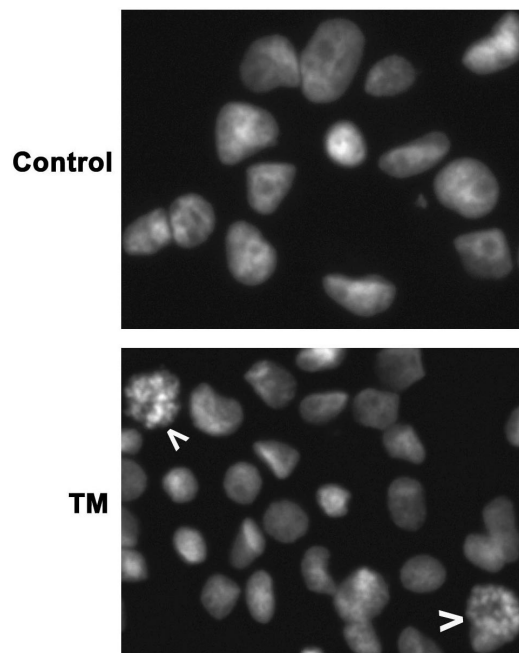


**Fig. 3** Tunicamycin-treated cells undergo nuclear fragmentation. Capillary endothelial cells cultured and synchronized as in Materials and Methods. The nuclei from control and tunicamycin (1  $\mu\text{g/ml}$ ) treated cells were stained with Hoechst 33528 (10  $\mu\text{g/ml}$  in PBS, pH 7.2) and examined them under a fluorescence microscope. Arrows indicated the site of nuclear fragmentation.

### Raman spectroscopy of control and tunicamycin-treated capillary endothelial cells

About one-third of newly synthesized proteins translocate to the lumen of the ER where they are subject to post-translational modifications and folded into correct 3D structures before being targeted to various cellular organelles or transported to the surface of the cell. This process is highly sensitive to alterations in the ER luminal environment.

Among the variety of insults that disrupt protein folding in the ER lumen and activate the UPR, the most notable chemical inducer is the protein *N*-glycosylation inhibitor tunicamycin. There is no established analytical tool currently available to detect the ER stress-mediated UPR. Because Raman spectroscopy targets protein conformation, we have used it here to assess the cellular milieu following tunicamycin treatment. The spectra were collected from capillary endothelial cells after culturing in the presence or absence of tunicamycin (1  $\mu\text{g/ml}$ ) for 3 and 12 h. Figure 4A displays the spectrum in cells cultured for 3 h in the absence of tunicamycin. The inset is an enlarged 1700–1600  $\text{cm}^{-1}$  region showing bands at 1694, 1684, and 1672  $\text{cm}^{-1}$ , respectively. These bands originate mainly from the C=O stretch of mono-substituted amides as in proteins [29,32]. The spectral band near 1650  $\text{cm}^{-1}$  is characteristic of proteins in their secondary and/or tertiary structures (the amide I band). For example, Raman spectra of  $\alpha$ -helices peak around 1655  $\text{cm}^{-1}$ , but those of  $\beta$ -sheets peak around 1670  $\text{cm}^{-1}$  [32]. The

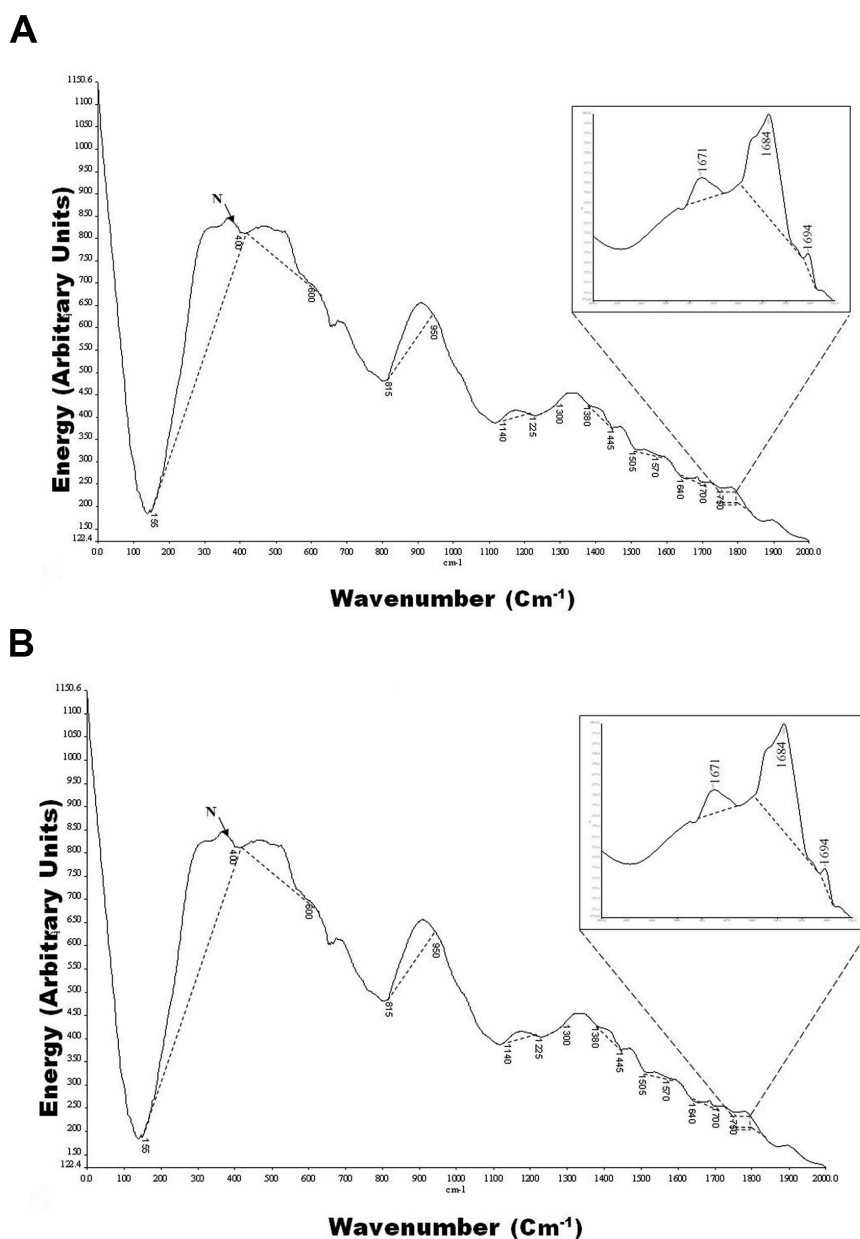


**Fig. 4** Raman spectroscopy of capillary endothelial cells after 3 h of culturing in the absence or presence of tunicamycin. Capillary endothelial cells were synchronized and cultured in absence or presence of tunicamycin (1  $\mu\text{g/ml}$ ) for 3 h. At the end of the incubation period, the cells were removed from culture dishes with a short trypsinization, washed with PBS, pH 7.4, and suspended in 70 % aqueous ethanol (v/v). After 2 days at  $-20\text{ }^{\circ}\text{C}$ , the cells were recovered by a short centrifugation and the pellets containing  $3.7 \times 10^4$  cells were placed in a microcup. Ethanol was evaporated at room temperature and the Raman spectra were recorded in an R 2001 Raman Systems Spectrophotometer from Ocean Optics. Cells were scanned in the  $2800\text{--}0\text{ cm}^{-1}$  range, at integration 400, average 1 and box 15. Raman bands were quantified using Spectrum 1000 software from Perkin Elmer. The enlarged  $1700\text{--}1600\text{ cm}^{-1}$  region, characteristic of the C=O amide stretch, appears in the inset. The arrow points to the band used to normalize the spectra. (A): spectra from control cells; (B): spectra from cells treated with tunicamycin.

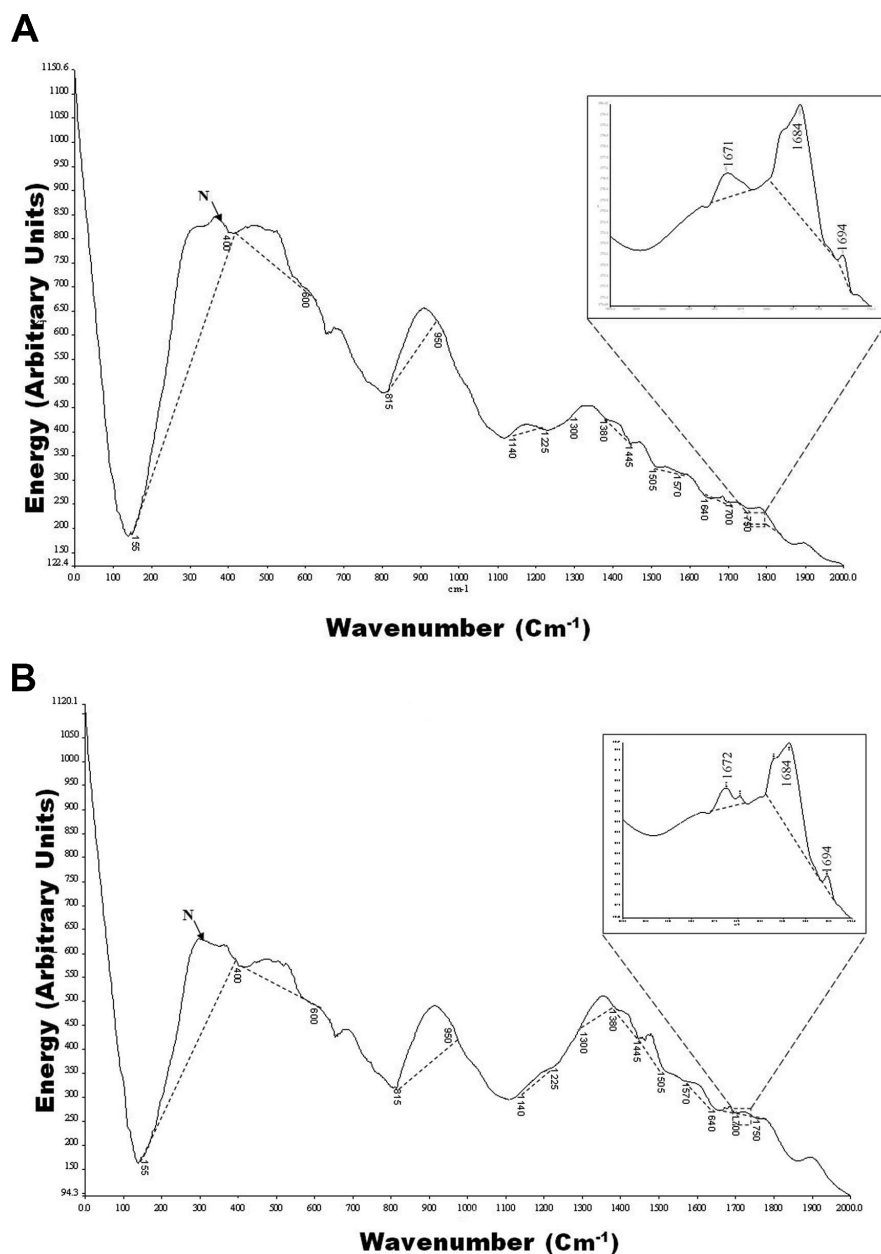


**Fig. 5** Raman spectroscopy of capillary endothelial cells after 12 h of culturing in the absence or presence of tunicamycin. Capillary endothelial cells were synchronized and cultured in the absence or presence of tunicamycin (1  $\mu\text{g}/\text{ml}$ ) for 12 h. At the end of the incubation period, the cells were removed from culture dishes with a short trypsinization, washed with PBS, pH 7.4, and suspended in 70 % aqueous ethanol (v/v). After 2 days at  $-20\text{ }^{\circ}\text{C}$ , the cells were recovered by a short centrifugation and the pellets containing  $3.7 \times 10^4$  cells were placed in a microcup. Ethanol was evaporated at room temperature, and the Raman spectra were recorded in an R 2001 Raman Systems Spectrophotometer from Ocean Optics. Cells were scanned in the  $2800\text{--}0\text{ cm}^{-1}$  range, at integration 400, average 1 and box 15. Raman bands were quantified using Spectrum 1000 software from Perkin Elmer. Inset shows the  $1700\text{--}1600\text{ cm}^{-1}$  region characteristic of the C=O amide stretch. (A): spectra from control cells; (B): spectra from cells treated with tunicamycin.

band at 1672  $\text{cm}^{-1}$  in the spectra obtained in this study may originate from disordered  $\alpha$ -helices [32], but the ones at 1684 and 1694  $\text{cm}^{-1}$  certainly arise from completely disordered protein chains [32]. The intensities of these bands decrease significantly, when the cells are cultured in the presence of tunicamycin (Fig. 4B), the C=O moieties of their amide groups are not energetically suitable to absorb infrared light in the 1700–1600  $\text{cm}^{-1}$  region.

The Raman spectra of cells cultured for 12 h without tunicamycin show typical protein bands; those in the 1700–1600  $\text{cm}^{-1}$  region are enlarged in the inset (Fig. 5A). The intensities of these bands, however, decrease significantly when the cells are cultured in the presence of tunicamycin (1  $\mu\text{g}/\text{ml}$ ; Fig. 5B). Table 1 summarizes the details of these experimental results.

**Table 1** Intensities of Raman spectral bands in the 1700–1600  $\text{cm}^{-1}$  region in capillary endothelial cells in the presence or absence of tunicamycin.

Sample	Wave number ( $\text{cm}^{-1}$ )	Band area* (absorbance)	S.D.	Change in band area (%)
3 h (no tuni)	1694	0.5400	0.0787	
3 h (1 $\mu\text{g}/\text{ml}$ tuni)		0.3600	0.0759	33.33 ↓
12 h (no tuni)	"	0.6880	0.1610	
12 h (1 $\mu\text{g}/\text{ml}$ tuni)		0.4615	0.0710	32.92 ↓
3 h (no tuni)	1684	0.1500	0.0022	
3 h (1 $\mu\text{g}/\text{ml}$ tuni)		0.1190	0.0022	20.63 ↓
12 h (no tuni)	"	0.8104	0.1181	
12 h (1 $\mu\text{g}/\text{ml}$ tuni)		0.4856	0.0477	40.08 ↓
3 h (no tuni)	1672	0.0408	0.0076	
3 h (1 $\mu\text{g}/\text{ml}$ tuni)		0.0237	0.0047	41.85 ↓
12 h (no tuni)	"	0.0607	0.0010	
12 h (1 $\mu\text{g}/\text{ml}$ tuni)		0.0271	0.0084	55.39 ↓

tuni = tunicamycin

\*Expressed in arbitrary units determined by Spectrum 1000 Software.

S.D. = standard deviation from the mean of three different samples analyzed in duplicate. Spectra were normalized using the Raman spectroscopy band at 400–155  $\text{cm}^{-1}$  which did not change.

## DISCUSSION

In malignant breast tissue, the intratumoral endothelial cell proliferation rate is higher than that of the surrounding breast [37]. The central importance of angiogenesis and the current understanding of blood vessel formation are leading the way to develop therapies to interrupt this process. We have recently observed that treatment of capillary endothelial cells with tunicamycin causes cell cycle arrest in G1 [24,34]. Also, (i) tunicamycin inhibits angiogenesis *in vivo* and reduces a double- and triple-negative breast tumor growth in nude mice; (ii) inhibition is stable under tumor microenvironment and (iii) is irreversible by exogenous VEGF<sub>165</sub>. The study we have presented here with tunicamycin has offered an enormous possibility for developing a new drug regimen for treating breast cancer. The outcome is from a central hypothesis that tunicamycin inhibits angiogenesis (both *in vitro* and *in vivo*) and built on the confidence that inhibition of capillary endothelial cell proliferation is by arresting cells in G1 [28].

*N*-linked glycoproteins have been found to play an important role in angiogenesis [23–27,38,39]. We have observed that proliferation of capillary endothelial cells as well as the capillary lumen formation is up-regulated when the cells are treated with 8Br-cAMP [30,35,40]. Up-regulated mannosyl-phospho dolichol synthase (DPMS) activity increases the synthesis and turnover of Glc<sub>3</sub>Man<sub>9</sub>GlcNAc<sub>2</sub>-PP-Dol (lipid-linked oligosaccharide, LLO) and consequently the *N*-glycosylation of Factor VIIIc

(eFVIIIc), enhancing angiogenesis [41]. Tunicamycin, a glucosamine-containing pyrimidine nucleoside and a competitive inhibitor of GPT, inhibits protein *N*-glycosylation by blocking the LLO synthesis in the ER [42]. Consequently, the glycoproteins are not folded and caused an accumulation of mis- or unfolded glycoproteins in the ER. This saturation of the ER folding capacity induces ER stress and activates ER-specific adaptive response, the UPR [43]. The underlying mechanism of UPR induced by ER stress could indirectly impede cell cycle progression by interfering with the proper maturation of growth factor receptors or other modulators of mitogenic signaling. Alternatively, ER stress may directly induce checkpoint response and prevent cells from completing their cell division cycle [44].

The study we have presented here clearly establishes that tunicamycin inhibits capillary endothelial cell proliferation, and, more importantly, the treatment would not allow the cells to regain their proliferative status when tunicamycin is withdrawn from the culture media. The clonogenic assay (Fig. 2) supports unequivocally that even a short (i.e., 3 h) exposure of tunicamycin is fatal and prevents the capillary endothelial cells going back to proliferation.

Another milestone is that using Raman spectroscopy we could confidently explain that the development of ER stress-mediated UPR is due to inhibition of *N*-glycosylation of proteins. In fact, it is due to intracellular protein denaturation. The Raman bands characteristic of the C=O stretch of amide groups are typical of disordered protein chains; even the band at 1672 cm<sup>-1</sup>, which should arise from a disordered helix [32]. This demonstrates that proteins synthesized by the capillary endothelial cells under the experimental condition have disordered structures. In the presence of tunicamycin, these structures are altered to ones that no longer absorb infrared light at the same frequency, which is an indication of protein denaturation. This damage was demonstrated by the reduced band intensity of the C=O amide stretch (1700–1600 cm<sup>-1</sup> region), which ranges from 20.63 % at 1684 cm<sup>-1</sup> in cells cultured for 3 h in the presence of tunicamycin to 55.39 % at 1673 cm<sup>-1</sup> in cells cultured for 12 h in its presence. The results, therefore, demonstrate that in the presence of tunicamycin, a significant number of newly synthesized proteins do not assume their normal, secondary, and/or tertiary conformations. Consequently, they cannot perform their normal roles in maintaining cellular physiology. This induces apoptosis by UPR signaling caused by the ER stress.

## ACKNOWLEDGMENTS

The work was supported in part by grants from Susan G. Komen for the Cure BCTR0600582 (DKB), NIH/NCRR/RCMI grant G12-RR03035 (KB), and by Scholarly Release from Purdue University Calumet (MOL). The authors also greatly acknowledge the contributions of the graphic designers Amarilys Irizarry and Amitava Banerjee.

## REFERENCES

1. R. G. Spiro. *Glycobiology* **12**, 43R (2002).
2. M. E. Taylor, K. Drickamer. *Introduction to Glycobiology*, Oxford University Press, Oxford (2003).
3. C. Wang, M. Eufemi, C. Turano, A. Giartosio. *Biochemistry* **35**, 7299 (1996).
4. C. J. Bosques, S. M. Tschampel, R. J. Woods, B. Imperiali. *J. Am. Chem. Soc.* **126**, 8421 (2004).
5. A. Helenius, M. Abei. *Annu. Rev. Biochem.* **73**, 1019 (2004).
6. K. A. Karlsson. *Curr. Opin. Struct. Biol.* **5**, 622 (1995).
7. D. M. Underhill. *Eur. J. Immunol.* **33**, 1767 (2003).
8. M. Colmenares, A. L. Corbi, S. J. Turco, L. Rivas. *J. Immunol.* **172**, 1186 (2004).
9. A. E. Smith, A. Helenius. *Science* **304**, 237 (2004).
10. C. Slawson, R. J. Copeland, G. W. Hart. *Trends Biochem. Sci.* **35**, 547 (2010).
11. P. R. Crocker. *Curr. Opin. Struct. Biol.* **12**, 609 (2002).
12. J. D. Esko, S. B. Selleck. *Annu. Rev. Biochem.* **71**, 435 (2002).

13. J. B. Lowe. *Immunol. Rev.* **186**, 19 (2002).
14. G. A. Rabinovich, L. G. Baum, N. Tinari, R. Paganelli, C. Natoli, F. T. Liu, S. Iacobelli. *J. Immunol.* **151**, 4764 (2002).
15. D. K. Banerjee. *Science* **218**, 569 (1982).
16. A. Cazet, S. Julien, M. Bobowski, J. Burchell, P. Delannoy. *Breast Cancer Res.* **12**, 204 (2010).
17. S. Hakomori. *Cancer Res.* **56**, 5309 (1996).
18. T. Muramatsu. *Glycobiology* **3**, 291 (1993).
19. H. H. Wandall, O. Blixt, M. A. Tarp, J. W. Pedersen, E. P. Bennett, U. Mandel, G. Ragupathi, P. O. Livingston, M. A. Hollingsworth, J. Taylor-Papadimitriou, J. Burchell, H. Clausen. *Cancer Res.* **70**, 1306 (2010).
20. N. Taniguchi, K. Honke, M. Fukuda. *Handbook of Glycosyltransferases and their Related Genes*, Springer, Tokyo (2002).
21. S. Bernales, F. R. Papa, P. Walter. *Annu. Rev. Cell Dev. Biol.* **22**, 487 (2006).
22. M. Schroder, R. J. Kaufman. *Annu. Rev. Biochem.* **74**, 739 (2005).
23. T. Tiganis, D. D. Leaver, K. Ham, A. Friedhuber, P. Stuart, M. Dziadek. *Exp. Cell Res.* **198**, 191 (1992).
24. D. K. Banerjee, J. A. Martinez, K. Baksi. In *Angiogenesis: Basic Science and Clinical Applications*, M. E. Maragoudakis, E. Papadimitrou (Eds.), pp. 281–302, Transworld Research Network, Trivandrum, Kerala, India (2007).
25. M. Nguyen, J. Folkman, J. Bischoff. *J. Biol. Chem.* **267**, 26157 (1992).
26. M. Nguyen, N. A. Strubel, J. Bischoff. *Nature* **365**, 267 (1993).
27. R. Pili, J. Chang, R. A. Partis, R. A. Mueller, F. J. Chrest, A. Passaniti. *Cancer Res.* **55**, 2920 (1995).
28. A. Banerjee, J. Y. Lang, M.-C. Hung, K. Sengupta, S. K. Banerjee, K. Baksi, D. K. Banerjee. *J. Biol. Chem.* **286**, 29127 (2011).
29. E. A. Carter, H. G. M. Edwards. “Biological applications of Raman spectroscopy”, in: *Infrared and Raman Spectroscopy of Biological Materials*, H.-U. Gremlich, Y. Bing (Eds.), pp. 421–475, Marcel Dekker (2001).
30. M. D. Keller, E. M. Kanter, A. Mahadevan-Jansen. *Spectroscopy* **21**, 1133 (2006).
31. S. Verrier, I. Notingher, J. M. Polak, L. L. Hench. *Biopolymers* **74**, 157 (2004).
32. S. U. Sane, S. M. Cramer, T. M. Przybycien. *Anal. Biochem.* **269**, 255 (1999).
33. D. K. Banerjee, R. L. Ornberg, M. B. H. Youdim, E. Heldman, H. B. Pollard. *Proc. Natl. Acad. Sci. USA* **82**, 4702 (1985).
34. J. A. Martinez, I. Torres-Negron, L. A. Amigo, D. K. Banerjee. *Cell Mol. Biol.* **45**, 137 (1999).
35. J. A. Martinez, J. J. Tavares, C. M. Oliveira, D. K. Banerjee. *Glycoconjugate J.* **23**, 209 (2006).
36. C. Wang, G. L. Zhou, S. Vedantam, P. Li, J. Field. *J. Cell Sci.* **121**, 2913 (2008).
37. R. K. Vartanian, N. Weidner. *Am. J. Pathol.* **144**, 1188 (1994).
38. D. K. Banerjee, M. Vendrell-Ramos. *Ind. J. Biochem. Biophys.* **30**, 389 (1993).
39. C. M. Oliveira, D. K. Banerjee. *J. Cell Physiol.* **144**, 467 (1990).
40. S. K. Das, S. Mukherjee, D. K. Banerjee. *Mol. Cell Biochem.* **140**, 49 (1994).
41. D. K. Banerjee, C. M. Oliveira, J. J. Tavares, V. N. Katiyar, S. Saha, J. A. Martinez, A. Banerjee, A. Sanchez, K. Baksi. *Adv. Exp. Med. Biol.* **705**, 453 (2011).
42. R. Kornfeld, S. Kornfeld. *Annu. Rev. Biochem.* **54**, 631 (1985).
43. K. Zhang, R. J. Kaufman. *J. Biol. Chem.* **279**, 25935 (2004).
44. J. W. Brewer, L. M. Hendershot, C. J. Sherr, J. A. Diehl. *Proc. Natl. Acad. Sci. USA* **96**, 8505 (1999).